World Academy of Science, Engineering and Technology
International Journal of Energy and Power Engineering
Vol:10, No:12, 2016

Online Electric Current Based Diagnosis of Stator Faults on Squirrel Cage Induction Motors

Alejandro Paz Parra, Jose Luis Oslinger Gutierrez, Javier Olaya Ochoa

***Abstract*—**In the present paper, five electric current based methods to analyze electric faults on the stator of induction motors (IM) are used and compared. The analysis tries to extend the application of the multiple reference frames diagnosis technique. An eccentricity indicator is presented to improve the application of the Park's Vector Approach technique. Most of the fault indicators are validated and some others revised, agree with the technical literatures and published results. A tri-phase 3hp squirrel cage IM, especially modified to establish different fault levels, is used for validation purposes.

***Keywords*—**Motor fault diagnosis, induction motor, MCSA, ESA, Extended Park´s vector approach, multiparameter analysis.

I. Introduction

ELECTRIC machinery is the main mechanic power source in modern industry in many productive areas; IMs represent more than 90% of the electrical motors in productive processes. Therefore, the maintenance of the reliability for the operation of the IM is an important key in many industrial applications [1]-[3].

There are four parts of the IM structure susceptible to failure, which are the stator, rotor, bearings and other miscellaneous components such as the electric power supply or the cooling fan. Anyone of these parts is susceptible to faults caused by multiple mechanical or electrical efforts like mechanical friction, low lubrication on mobile parts, contamination or poor quality of the electric power supply. A rated IM faults distribution by zone is represented in Fig. 1 [1], [4], [5].

Stator faults can be classified into two groups according to the point of occurrence: Windings or iron core faults. The main causes of stator core iron damage are overheating, vibrations, circulating current heating or poor cooling, while winding faults are associated with insulation loss. Winding faults are widely considered more common than stator core ones [4].

Alejandro Paz P. is a professor of the Department of Electronics and Computer Science at Pontificia Universidad Javeriana, Cali, Colombia (e-mail: apaz@javerianacali.edu.co).

Jose Luis Oslinger is a professor of the Electric and Electronics Engineering School & researcher of the Research Group in Energy Conversion CONVERGÍA at Universidad del Valle, Cali, Colombia (e-mail: jose.oslinger@correounivalle.edu.co).

Javier Olaya O. is a professor of the Industrial Engineering and Statistics School & researcher of the Research Group in Applied Statistics INFERIR at Universidad del Valle. Cali. Colombia (e-mail: jolaya@correounivalle.edu.co).

II. Electric Current Based Diagnostic Techniques for Stator Faults

There are many documented techniques for stator faults detection in the technical literature review; some of them are based in the direct visual offline inspection of motor windings, as defined by the IEEE STD 62.2-2004 [6]. However, the most common faults could remain undetected by visual inspection techniques overall, particularly when the fault is inside of the cooper wire insulation that forms the winding (Inter turn faults).

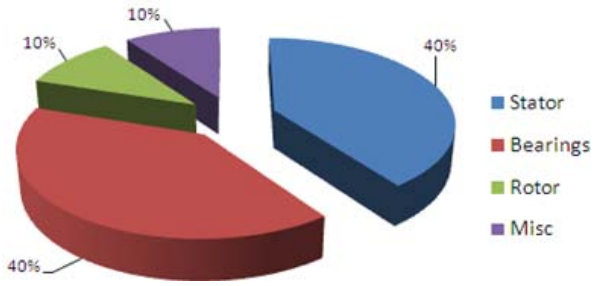

Fig. 1 IM faults distribution by zone [1]

As an alternative to visual inspection techniques, other offline tests are clearly documented, including a high voltage test for insulation monitoring as defined by IEEE STD 43 – 2000 [7] and IEEE STD 112- 2004 [8]. This kind of test is never recommended because of the high electromagnetic strength suffered by the insulation material that can seriously affect its useful life. The application of these essays is limited to the cases when the motor is re-started after a long time out of service or when it is received from the fabricant.

Online test for condition monitoring of the insulation becomes necessary to reduce the fault probability on the time interval when the motor condition remains unobserved. Most of the faults remain undetected and evolve quickly to a catastrophic condition in the time interval between two periodic visual or electric inspections, and tests are unable to establish a fault probability to program the next direct inspection of the winding. Main online techniques are based on the analysis of the current, voltages or electric power in the time or frequency domain, as defined below:

A. Motor Current Signature Analysis (MCSA)

MCSA is based on the electromagnetic effect from the high fault current generated for a fault condition. When an insulation loss occurs between two wires of the same winding coil, a high closed circuit current circulates generating a pulsating electromagnetic field located in the short circuited

slot [9]. Because the motor keeps moving, an induced electromotive force (EMF) appears in the rotor winding, and consequently, a high pulsating current is induced. The reflected pulse from the induced rotor current is detectable in the stator current as harmonic sidebands components at both sides of the stator current in the frequency domain spectra. Frequencies associated with an inter-turn stator fault are defined by [10]:

$$f_{sk} = \left[\frac{n}{p}(1-s) \pm k\right] f_s \tag{1}$$

where k is the order harmonic k=1,3,5...; n=1,2,3...(2p-1). p is the pair of magnetic poles, f_s is the main frequency of the power supply and s is the rotor slip.

B. Electric Power Spectral Analysis (ESA)

Is a similar technique to the MCSA, but the harmonic sidebands are sought in the spectral analysis of the electric power. Electric power harmonics are the same defined for MCSA [12].

The electric power spectral analysis tries to avoid the distortion on the stator current waveform caused by electric drives.

The instantaneous electric power is obtained as:

$$p(t) = v_a(t)i_a(t) + v_b(t)i_b(t) + v_c(t)i_c(t) \tag{2}$$

where: v_a, v_b, v_c, i_a, i_b and i_c are the instantaneous values of the phase voltages and line currents in the stator.

Instantaneous electric power spectral analysis is a useful diagnosis technique, even under unbalanced or misalignment mechanical load conditions [18].

C. Negative Sequence Current

If the IM is considered as a linear system, there exists the possibility of replacing the system of the three-phase unbalanced voltages and currents for three equivalent balanced systems: positive, negative and zero sequence. When the power supply is balanced, the electrical faults in the stator can be related directly to asymmetry in the equivalent electromagnetic circuit and in the symmetrical components of induced voltages, currents, and impedance [12], [15].

Voltage and current symmetrical components are related with the phase voltages and currents through Fortescue's transformation:

$$\begin{bmatrix} V_o \\ V_p \\ V_n \end{bmatrix} = \begin{bmatrix} 1 & 1 & 1 \\ 1 & a & a^2 \\ 1 & a^2 & a \end{bmatrix} \begin{bmatrix} V_a \\ V_b \\ V_c \end{bmatrix}$$
$$\begin{bmatrix} I_o \\ I_p \\ I_n \end{bmatrix} = \frac{1}{\sqrt{3}} \begin{bmatrix} 1 & 1 & 1 \\ 1 & a & a^2 \\ 1 & a^2 & a \end{bmatrix} \begin{bmatrix} I_a \\ I_b \\ I_c \end{bmatrix} \tag{3}$$

where: Va, Vb and Vc: Are the phasors representing the phase voltages of the stator. Ia, Ib and Ic: Are the phasors of the line currents in the stator and **a** is a complex number equivalent to: $a = e^{j\frac{\pi}{3}}$.

Under balanced supply and healthy motor conditions, the negative sequence components of the voltage and current must be zero, but under unbalanced or non-symmetric motor operation condition there's a variation in the negative sequence current that can be used for diagnostic purposes.

D. Park's Vector Approach (PVA)

Park's vector approach is a technique introduced by Antonio João Marques Cardoso in 1991 [5], and later extended to multiple faults diagnosis on IM. This technique combines the information from the three phase currents in two equivalent currents in the reference frame obtained from Park's transformation.

The expression for the transformation is presented in [13], [14]:

$$i_d = \sqrt{\frac{2}{3}} i_a - \frac{1}{\sqrt{6}} i_b - \frac{1}{\sqrt{6}} i_c$$
$$i_q = \frac{1}{\sqrt{2}} i_b - \frac{1}{2} i_c \tag{4}$$

where: i_a, i_b and i_c are the instantaneous values of the line currents in the stator. i_d, i_q are the instantaneous values of the direct and quadrature axes in Park´s transformation.

Additionally, the expression for electric equivalent current module is:

$$\left|i_p\right| = \left|i_d + j i_q\right| = \sqrt{i_d^2 + i_q^2} \tag{5}$$

When the motor operates in a normal condition, the three currents form an approximately balanced system. Hence, axes d and q currents can be expressed as:

$$i_d = \frac{\sqrt{6}}{2} I \times Sin(\omega t)$$
$$i_q = \frac{\sqrt{6}}{2} I \times Sin\left(\omega t - \frac{\pi}{2}\right) \tag{6}$$

where: I: Is the amplitude of the wave of electric current in the stator and ω is the angular frequency of the voltage and current.

In the complex Gaussian plane representation, the i_p vector describes a perfect circumference when the currents are adequately balanced in magnitude and phase, as shown in Fig. 2.

In a faulty condition, unbalanced currents circulate and the shape of the i_p vector becomes distorted and the perfect circumference becomes in an ellipse, as shown in Fig. 3.

E. Extended Park's Vector Approach (EPVA)

EPVA explores the spectral analysis of the module of the Park´s vector [12].

Under asymmetrical conditions caused by unbalanced power supply or stator winding faults, the magnitude of the Park´s vector changes from a constant value to a harmonically variable value with two main spectral components: A constant component or DC value, and one Fourier harmonically variable value at twice of the supply frequency $2f_s$, which is associated with the negative sequence current from the unbalanced current system, as shown in Fig. 4.

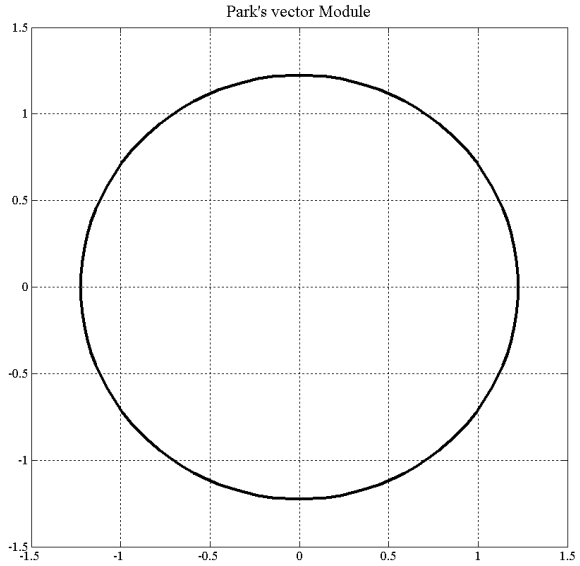

Fig. 2 Complex vector representation of the i_p current in p.u. for a healthy motor

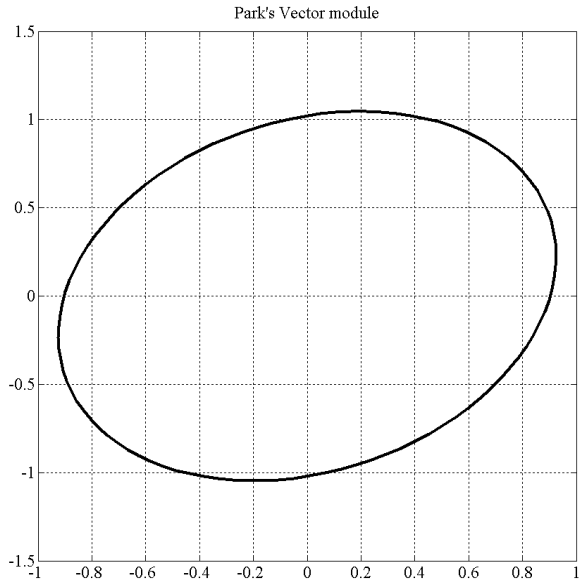

Fig. 3 Complex vector representation of the i_p current in p.u. for unhealthy motor

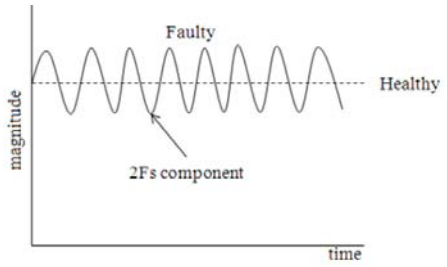

(a)

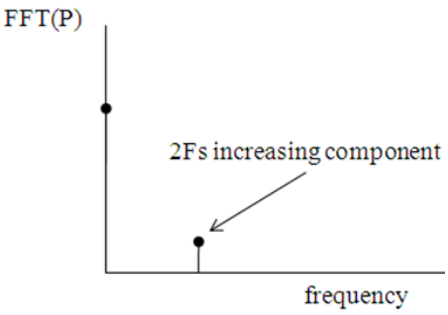

(b)

Fig. 4 Spectral harmonic components of the Park's vector: (a) In time domain and (b) in frequency domain under faulty condition

There could be another spectral component associated with harmonic current components from the stator and rotor slots, but these others have the least significance in the spectral analysis or could be minimized with adequate statistical techniques to reduce the influence of electromagnetic noise, as defined by [19].

III. Experimental Assembly

The techniques described were experimentally verified in a three phase 3Hp NEMA B, 220V, 4 poles, 1740 RPM, IM. The motor winding was modified to allow the possibility for making external short circuits between two, five, 10 and 14 turns of the same coil, as shown in Fig. 5.

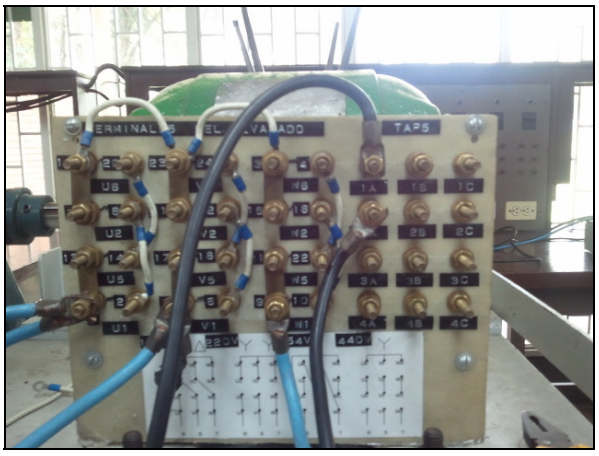

Fig. 5 Connection board of the motor under test

Voltages and currents in different faulty and healthy conditions were registered. Fault levels were introduced under no load, 50% load and rated load operation. The load condition was emulated with a DC generator used as an electric brake coupled to the motor axis, as shown in Fig. 6. A limiting resistance (R_f) of 0.14 Ohms for the fault current is used to avoid permanent damage to the stator winding.

IV. Results

A. Motor Current Signature Analysis MCSA

For the motor under test the Fourier harmonic components, defined as fault indicators for k=1,3,5 and n=1,2,3, f_s=60Hz and s=3.3% are: 27 Hz, 89 Hz, 118 Hz, 147 Hz, 209 Hz, 238 Hz, 267 Hz, 329 Hz, 358 Hz, and 387 Hz, respectively.

The amplitude of the electric current Fourier harmonics is expressed in decibels obtained from:

$$I_{dB} = 10 \times Log\left(\frac{I_{H-RMS}}{I_n}\right) \quad (7)$$

where: I_{H_RMS} is the harmonic electric current in Amperes - RMS value. I_n is the motor rated electric current in Amperes - RMS value.

In Fig. 6, the results of the comparative analysis for the main harmonic components under no load condition for healthy and faulty (14 turns short circuited) is shown. In Figs. 7 and 8, the same comparative analyses under 50% load and rated load condition is carried out.

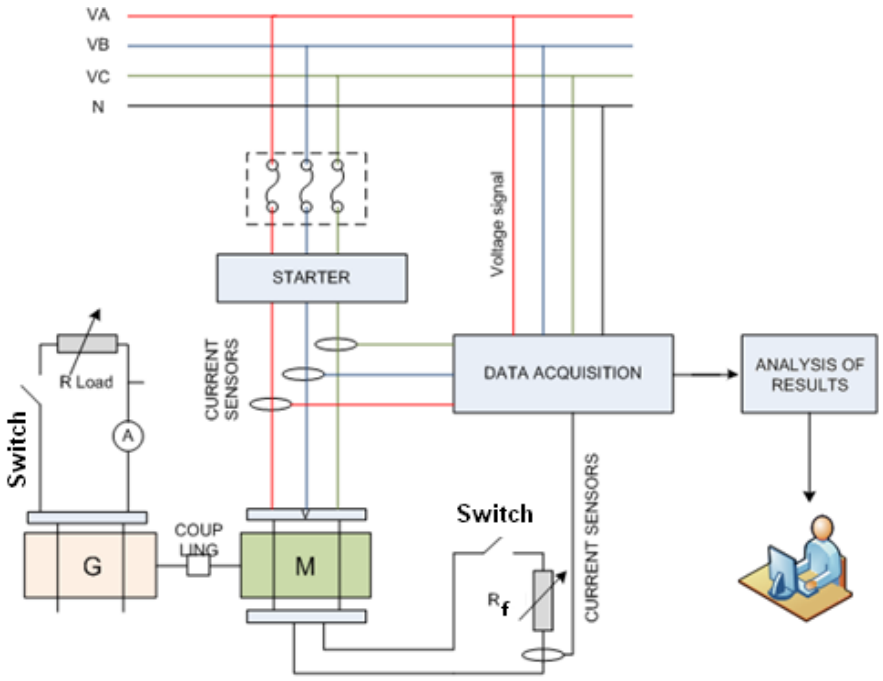

Fig. 6 Laboratory assemblies for fault emulation

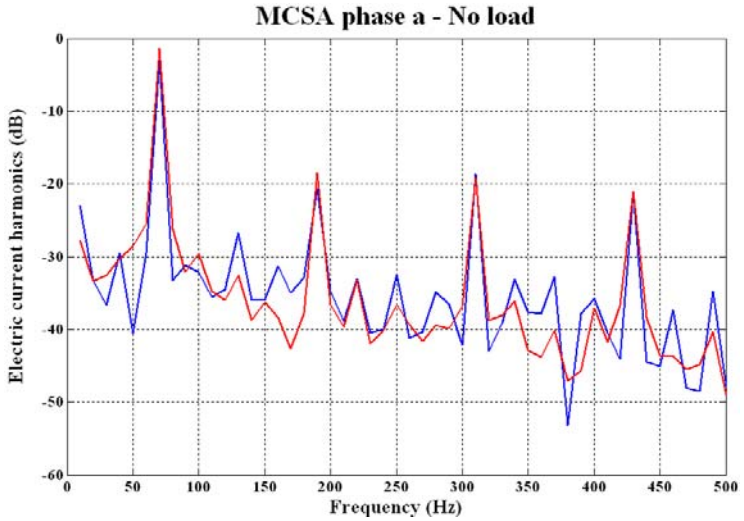

Fig. 7 Comparative analysis of MCSA (dB) applied to electric current phase a. Healthy motor (blue); Motor with 14 turns short circuited (red)

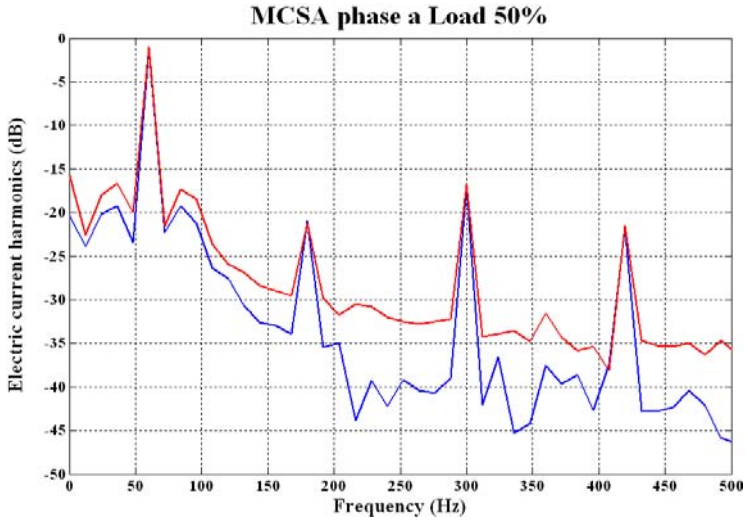

Fig. 8 Comparative analysis of MCSA (dB) applied to electric current phase a. Healthy motor (blue); Motor with 14 turns short circuited (red)

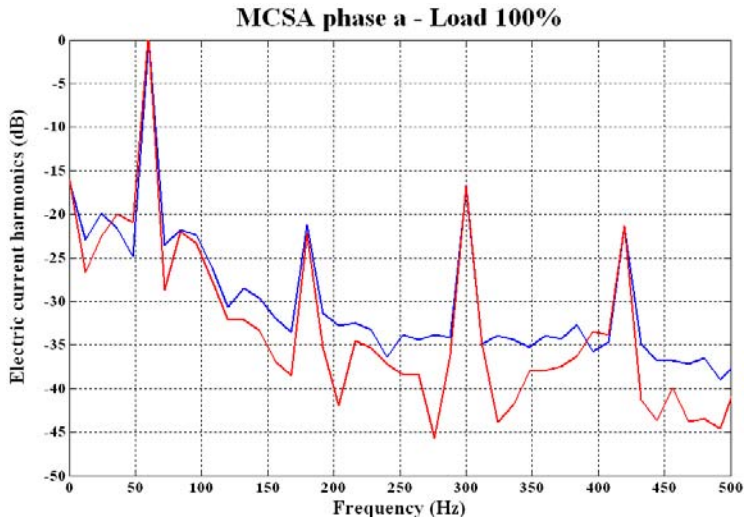

Fig. 9 Comparative analysis of MCSA (dB) applied to electric current phase a. Healthy motor (blue); Motor with 14 turns short circuited (red)

For the motor under test some variations in MCSA components was observed under fault conditions, but it does not establish a tendency and none of the severity factors can be obtained.

B. Electric Power Spectral Analysis ESA

For the motor under test, the electric power harmonic components are located at twice the frequency defined in MCSA, except by the main power component obtained in zero frequency. Frequency components used by analysis are: zero, 120 Hz, 240 Hz and 360 Hz, respectively.

The amplitude of the electric power harmonics is expressed in decibels obtained from:

$$P_{dB} = 10 \times Log\left(\frac{P_H}{S_n}\right) \quad (8)$$

where: P_H is the harmonic electric power in Watts. S_n is the motor rated apparent electric power defined from:

$$S_n = \sqrt{3} V_L I_L \quad (9)$$

where: V_L is the rated line voltage (220V) and I_L is rated line current (8.4A) of the IM.

In Fig. 10, the results of the comparative analysis for the main power harmonic components under no load condition for healthy and faulty (14 turns short circuited) is shown. There is a clearly recognizable relation between a power spectral $2f_s$ component and the electric short circuit fault. In Fig. 11, the $2f_s$ component evolution in the function of the fault level is analyzed; the use of this component as a fault indicator becomes plausible.

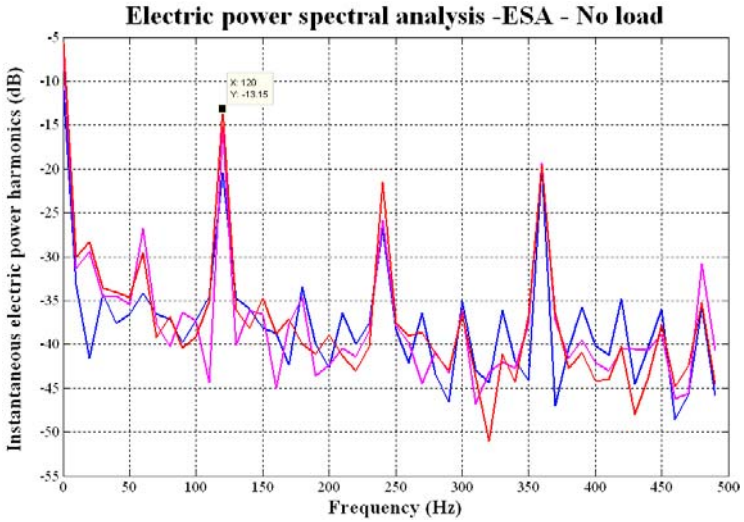

Fig. 10 Comparative analysis of ESA (dB) applied to electric power. Healthy motor (blue); Motor with 14 turns short circuited (red)

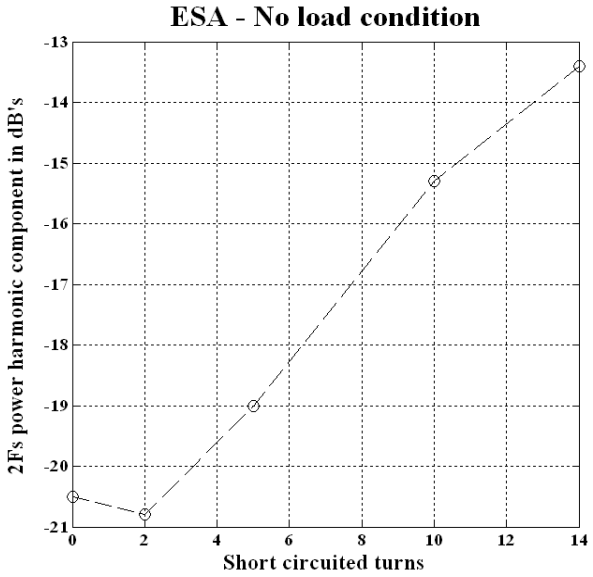

Fig. 11 Evolution of ESA $2F_s$ (dB) component in function of the number of short circuited turns

A severity factor can be associated to the amplitude in the dB of the $2f_s$ component in the electric power spectrum and the number of short circuited turns. In other harmonics components, a relationship between the amplitude and level fault becomes evident, as shown in Fig. 10. The $4f_s$ and $6f_s$ components evolve when the fault level increases.

C. Negative Sequence Current

With a voltage balanced power supply, the negative sequence components of the electric current under different fault conditions were measured and transformed by Fortescue's transformation to obtain the negative sequence current. Three different limiting resistances were used, and the results for the magnitude of the negative sequence current vs. the number of short circuited turns (n) are shown in Fig. 12. The negative sequence current becomes a reliable fault indicator as defined by [11], [14], [15], but for the motor under test, it becomes noticeable just for fault levels over five turns short circuited. The obtained results are consequent with the severity factor defined by [17].

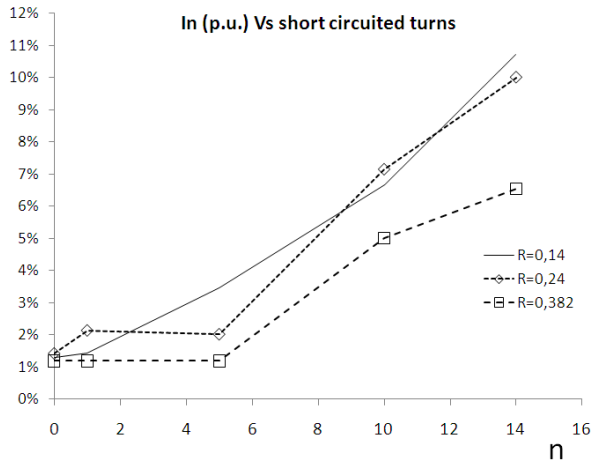

Fig. 12 Magnitude of the negative sequence current Vs number of short circuited turns with three different fault current limiting resistances

D. Park's Vector Approach

Park's vector expressed in p.u. is obtained as:

$$i_p(p.u.) = \frac{i_p(Amp)}{i_n(Amp)} \tag{10}$$

where I_p is the Park´s vector module and I_n is the rated current (8.4A) of the motor.

The Park's complex vector representation ($I_p=I_d+jI_q$) in healthy condition for the motor under test is shown in Fig. 13.

When different fault levels are induced, the complex vector representation becomes elliptical, as shown in Fig. 14. A clearly defined evolution with fault level is noticeable, as defined by Cardoso et al. [14].

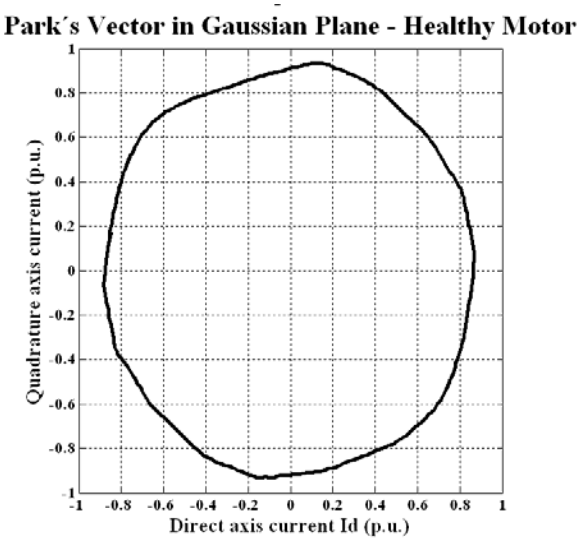

Fig. 13 Park's vector representation (p.u.) in Gaussian plane for healthy condition

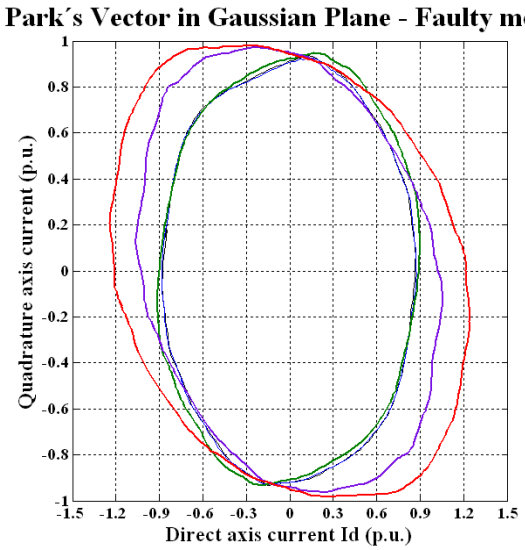

Fig. 14 Park's vector representation (p.u.) in Gaussian plane for faulty condition. The fault level is given by: Blue - two turns, green five turns, magenta 10 turns and red 14 turns short-circuited

In the time domain, the magnitude of complex Park´s vector for the motor under test is represented in Fig. 14. There is a clear variation on the amplitude with the fault level; it becomes clearly noticeable for more than five short circuited turns.

Novel techniques are being applied to identify variations in the shape of the Gaussian representation of the Park's Vector as presented by [16] but they are based in new signal processing techniques that are computationally expensive. A geometrical analysis allows us to propose two new indicators easier to compute:

There are two ways to measure the eccentricity of the ellipse generated for the fault condition, the first one is the eccentricity defined in analytic geometry of an ellipse given by:

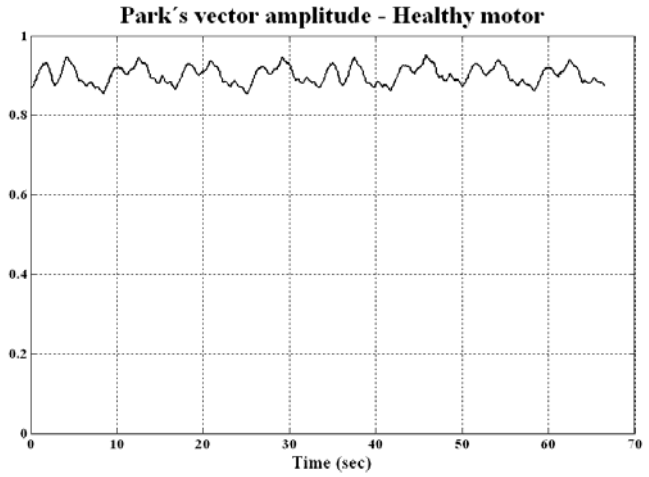

(a)

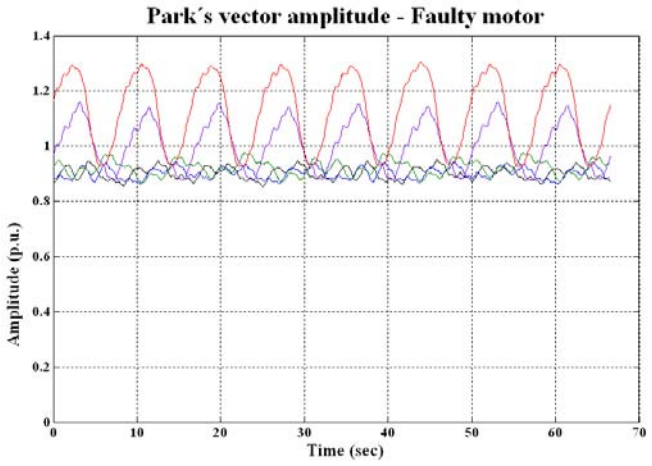

(b)

Fig. 15 Park's vector amplitude representation (p.u.) in time domain (a) For healthy condition and (b) Faulty condition. The fault level is given by: Blue - two turns, green five turns, magenta 10 turns and red 14 turns short-circuited

$$e_1 = \sqrt{1 - \left(b/a\right)^2} \tag{11}$$

where **b** and **a** are the lengths of minor and mayor axis of the ellipse and $\mathbf{e_1}$ is the eccentricity factor. In the Park´s vector approach is equivalent to the minimum and maximum values of the amplitude of the Park´s equivalent current I_p.

The other way is to use the relation between the maximum and minimum values of the Park´s equivalent current just like in the VSWR define for communication systems or in terms of analytic geometry the equivalent relation between the major and minor axis of the ellipse.

$$e_2 = \frac{a}{b} \tag{12}$$

where **b** and **a** are the lengths of minor and mayor axis of the ellipse and $\mathbf{e_2}$ is another eccentricity factor.

In Table I, these eccentricity factors are presented for different fault conditions. Either $\mathbf{e_1}$ or $\mathbf{e_2}$ can be used as fault indicators up than five short circuited turns.

TABLE I
ECCENTRICITY INDICATORS CALCULATED FOR THE MOTOR UNDER TEST FOR DIFFERENT FAULT CONDITIONS

n	Ip(media)	Ip(max)	Ip(min)	e_1	e_2
0	0.874	0.957	0.800	0.549	1.197
2	0.874	0.955	0.809	0.531	1.180
5	0.883	0.933	0.842	0.430	1.108
10	0.939	1.087	0.796	0.681	1.366
14	1.019	1.187	0.833	0.712	1.425

E. Extended Park's Vector Approach

The frequency domain representation of the Park's vector amplitude in healthy conditions is shown in Fig. 16. There is a highlighted zero frequency component and a negligible harmonic component.

The evolution of the high harmonic components is shown in Fig. 17. The zero frequency components are absent. It is clearly noticeable that there are three frequency components in 60 Hz, 120 Hz and 240Hz.

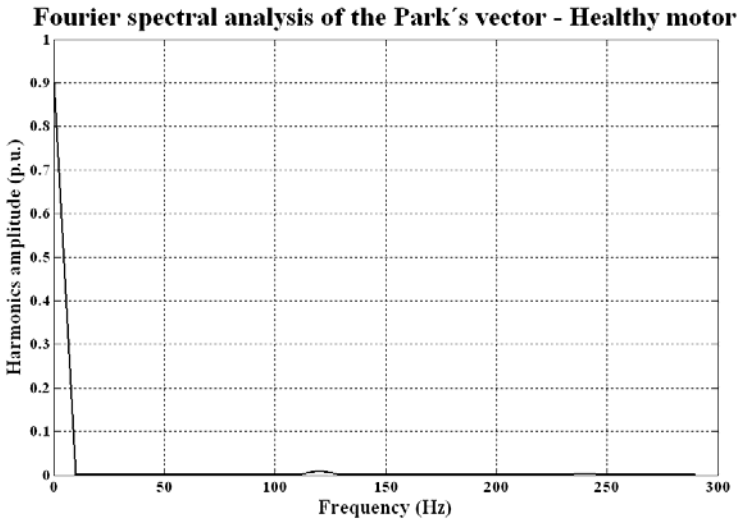

Fig. 16 Fourier spectral analysis of the Park's vector amplitude

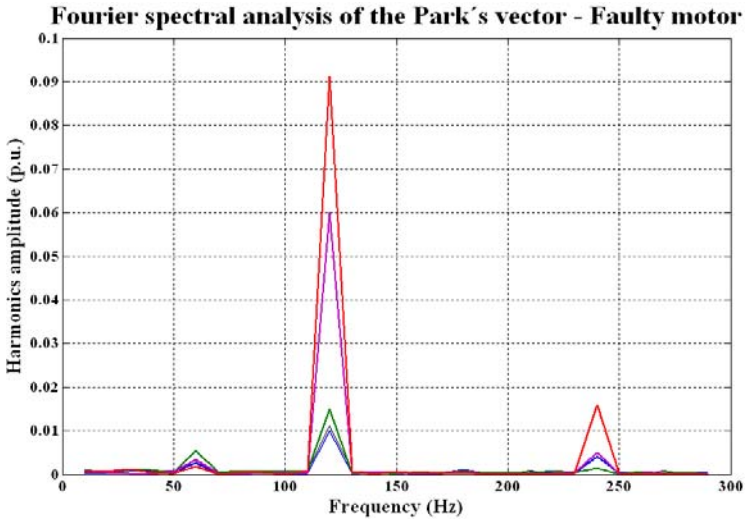

Fig. 17 Park's vector amplitude (p.u.) in frequency domain. The fault level is given by: Blue - 2 turns, green 5 turns, magenta 10 turns and red 14 turns short-circuited

The evolution of the $2f_s$ component as a percentage of the main Park´s vector component is used as a severity factor or fault indicator, as defined by Cardoso et al. [13].

V. CONCLUSIONS

The $2f_s$ component, defined by many authors, shows its utility for diagnostic purposes of stator electric faults. It becomes a reliable indicator of the ESA, PVA and EPVA techniques.

The two eccentricity factors proposed reduce the requirements of computational resources in the application of the PVA technique. They can be calculated with minus computational resources avoiding the requirements for digital signal process oriented to pattern recognition in the graphical representation of the Park´s vector in the Gaussian plane.

For the motor under test MCSA is not valid as a method for inter-turn electric fault detection and ESA, PVA, EPVA and negative sequence current becomes the most reliable of the techniques.

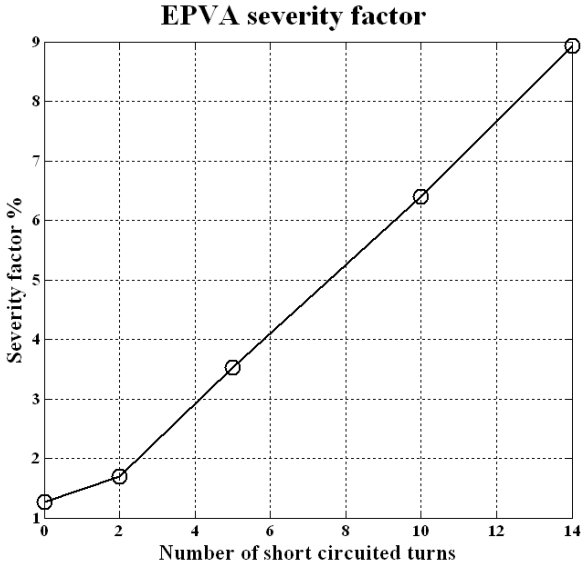

Fig. 18 Severity factor for stator inter-turn short-circuit fault Vs. number of short circuited turns

REFERENCES

[1] A. Paz Parra, M. C. Amaya Enciso, J. Olaya Ochoa and J. A. Palacios Peñaranda, "Stator fault diagnosis on squirrel cage induction motors by ESA and EPVA," Power Electronics and Power Quality Applications (PEPQA), 2013 Workshop on, Bogota, 2013, pp. 1-6.

[2] A. Siddique, G.S Yadava, B. Singh, "A review of stator fault monitoring techniques of induction motors," *IEEE Transactions on Energy Conversion*. Vol. 20, issue 1, pp. 106-114, March 2005.

[3] A. Bellini, F. Filippetti, C. Tassoni, G.A. Capolino, "Advances in diagnostic techniques for induction machines". *IEEE Transactions on Industrial Electronics*. Vol. 55, issue 12, p.4109-4126, Dec. 2008.

[4] A.J.M. Cardoso, "Diagnóstico de Avarias em motores de indução trifásicos," Coimbra, Portugal: Coimbra edições, 1991. Páginas. ISBN: 972-32-0452-5.

[5] Motor Reliability Working Group IEEE Industry Applications Society. "Report of Large Motor Reliability Survey of Industrial and Commercial Installations, Part I". *IEEE Transactions on Industry Applications*. Vol. IA-21, issue 4, p.853-864. July 1985.

[6] *IEEE Guide for Diagnostic Field Testing of Electric Power Apparatus – Electrical Machinery*, IEEE STD 62.2 – 2004, Dec. 2004.

[7] *IEEE Recommended Practice for Testing Insulation Resistance of Rotating Machinery*, IEEE STD 43 – 1974, May 1974.

[8] *IEEE Standard Test Procedure for Polyphase Induction Motors and Generators*, IEEE STD 112 – 2004, Nov. 2004.

[9] S.M.A. Cruz, A.J.M. Cardoso, "Multiple Reference Frames Theory: A New Method for the Diagnosis of Stator Faults in Three-Phase Induction Motors". *IEEE Transactions on Energy Conversion*. Vol. 20, issue 3, p.611-619. September 2005.

[10] S. Nandi, H. Toliyat, L. Xiaodong, "Condition Monitoring and Fault Diagnosis of Electrical Motors—A Review". *IEEE Transactions on Energy Conversion*. Vol. 20, number 4, p.197-204. December 2005.

[11] S. Legowski, A.H.M.U. Sadrul, A. Trzynadlowski, "Instantaneous power as a medium for the signature analysis of induction motors". *IEEE Transactions on Industry Applications*. Vol. 32, issue 4, p.904-909. Jul/Aug 1996.

[12] S. Bakhri, N. Ertugrul, W.L. Soong, M. Arkan, "Investigation of negative sequence components for stator shorted turn detection in induction motors". In *Proc. 2010 - 20th Australasian Universities Power Engineering Conference (AUPEC)*. pp. 1-6.

[13] S.M.A. Cruz, A.J.M. Cardoso, "Stator Winding Fault Diagnosis in Three-Phase Synchronous and Asynchronous Motors, by the Extended Park's Vector Approach", *IEEE Transactions on Industry Applications*. Vol. 37, issue 5, p. 1227 – 1233. Sept.-Oct. 2001.

[14] A.J.M. Cardoso, S.M.A. Cruz, D. S. B. Fonseca, "Inter-Turn Stator Winding Fault Diagnosis in Three-Phase Induction motors, by Park's Vector Approach," *IEEE Transactions on Energy Conversion*. Vol. 14, issue 3, p. 595-598. Sept. 1999.

[15] M. Bouzid, G. Champenois, "Accurate stator fault detection insensitive to the unbalanced voltage in induction motor". In *Proc. 2012 - XXth IEEE International Conference on Electric Machinery ICEM*. pp. 1543-1549.

[16] V.S. Dyonisios, D.M. Epaminondas, "Induction motor stator fault diagnosis technique using Park Vector Approach and complex wavelets". In *Proc. 2012 - XXth IEEE International Conference on Electric Machinery ICEM*. pp. 1543- 1549.

[17] C.H. De Angelo, G.R. Bossio, S.J. Giaccone, M.I. Valla, J.A. Solsona, G.O. Garcia, "Online Model-Based Stator-Fault Detection and Identification in Induction Motors," *IEEE Transactions on Industrial Electronics*. Vol. 56, no.11, pp.4671-4680, Nov. 2009.

[18] M. Drif, A.J.M. Cardoso, "Discriminating the Simultaneous Occurrence of Three-Phase Induction Motor Rotor Faults and Mechanical Load Oscillations by the Instantaneous Active and Reactive Power Media Signature Analyses," *IEEE Transactions on Industrial Electronics*, vol.59, no.3, pp.1630-1639, March 2012.

[19] Seungdeog Choi, B. Akin, M.M. Rahimian, Toliyat, H.A., "Performance-Oriented Electric Motors Diagnostics in Modern Energy Conversion Systems," *IEEE Transactions on Industrial Electronics*, vol. 59, no. 2, pp.1266-1277, Feb. 2012.

Alejandro Paz Parra Electrical Engineer from Universidad del Valle – Colombia in 1996 and M.Sc. in Electric Energy Generation Systems from the same institution in 2004. Ph.D in engineering of the Universidad del Valle - Colombia. His researching areas are closely related with rotating electric machinery modeling, simulation and diagnosis. Currently he is working like a full time professor of the Electronics and computer science departaament at the Pontificia Universidad Javeriana in Cali - Colombia. E-mail: apaz@javerianacali.edu.co.

Javier Olaya Ochoa Chemistry Technologist from Universidad del Valle – Colombia in 1977 and Statistical from the same institution in 1985. M.Sc. in Mathematical Sciences from Clemson University in 1997 and Ph.D. in Management Science from Clemson University in 2000. Currently is a Professor of the Industry Engineering and Statistics School of the Universidad del Valle - Colombia. His research field is the application of statistical methods in industry and environmental care applications. E-mail: jolaya@correounivalle.edu.co.

Jose Luis Oslinger Electrical Engineer from Technische Universität Graz Austria 1991 and Electrical Enginner from Universidad del Valle-Colombia in 1996. Ph.D in Electric engineering in 2007. Professor of Energy Conversion Area at the Electrical and Electronic Engineering School of the Universidad del Valle, Cali, Colombia. His research field is the analysis and modeling of energy conversion processes and its interaction with environmental processes and impact in Energy Conversion Research Group. E-mail: jose.oslinger@correounivalle.edu.co.